PIPES UNDER INTERNAL PRESSURE AND BENDING

Andrea Catinaccio, CERN, Geneva, Switzerland

Keywords

Thin and thick pipes under internal pressure with built-in open ends – coupling between internal pressure and curvature – lateral buckling/ instability – effects of isotropic or orthotropic material on curvature variation – composite laminate formulation – FEA simulations.

Abstract

This article covers the general behaviour of a straight uniform pipe, with built-in open ends, subject to internal pressure and in plane bending or curvature.
It is intended as a summary of the basic equations driving the unintuitive phenomena of bending and instability of pipes under internal pressure. The analysis covers in addition the investigation of opposite pressure stabilisation effects that can be observed in some orthotropic material pipes like composite pressure hoses.

INTRODUCTION

It has been shown by Haringx already in 1952 [2] and in several later publications [3,4] that a straight pipe with built-in ends can buckle laterally when the internal pressure reaches the Euler compression column buckling load. At that moment, the contained fluid exerts a lateral force on the deflected pipe; the magnitude of the force, acting towards the outside of the curve, is the product of the pressure by the cross-section multiplied by the curvature. If the pipe is not perfectly straight due to an initial bending, this coupling between the pressure and curvature is present since the very beginning. When the pressure rises inside the pipe, the coupling effects cause the pipe to bend more till a sudden large deflection will be reached at the Euler instability value. In a non-linear analysis approach, the effects of the ends constrained and the stress stiffening of the pipe will limit this deflection to finite values. This is confirmed in this study and applies to all isotropic material pipes.
The phenomenon is explained through simple analytical relations. It's shown to depend on the net longitudinal force on the pipe wall given by the expression $P = \pi / 4\, D^2 p\, (1-2\nu)$ with p internal pressure, where P is always positive, thus compressive, for Poisson ratio's ν never exceeding the value of ½ in isotropic materials.

But why in reality not all pipes are subject to this instability and when initially bent, some can decrease their curvature under internal pressure and get straight, thus stable?

It is shown here that for orthotropic material pipes the expression of the longitudinal force P still holds when ν is being replaced by the opportune Poisson ratio ν_{lc} in the longitudinal-circumferential directions. Since some orthotropic materials, like for instance reinforced pressure hoses and composite laminates, may have Poisson ratio's ν_{lc} well exceeding the value of ½, the longitudinal force can now become negative and thus tensile. This is confirmed by the finite element analysis detecting either straightening or increased bending of the pipe under pressure, depending on ν_{lc} above or below ½ .

Straightening effects based on Haigh's out of roundness analysis have been neglected in this article which covers the behaviour of pipes of relatively small curvature.

PROBLEM DEFINITION

Consider the pipe of Fig.(1) with built-in open ends, subject to lateral distributed load q and an internal pressure p.

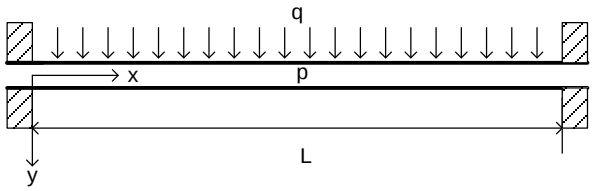

Fig.[1]: Open end pipe under internal pressure and lateral load q

For the equilibrium equations of the deflected pipe we have selected [5] an empty control element Fig.(2), in which the effects of the contained fluid are replaced by the internal pressure p acting on the wall. The distributed load q includes the fluid weight in case the pipe is horizontal.
Although several formulations are possible [2] this control element is particularly convenient to check the assumptions of the Finite Element Model developed further on.

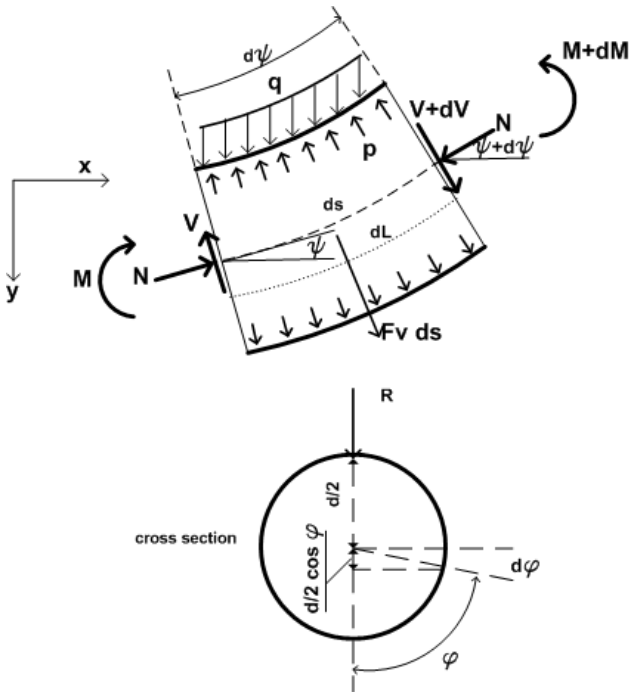

Fig.[2]: equilibrium control element

In the following analysis we restrict ourselves to cylindrical pipes. The notation *l, c, r,* used further on, denote the longitudinal, circumferential and radial directions.

Fig.(2) shows a segment *dL* of a slightly deflected pipe and its cross section. The length along the pipe inner surface varies from *R*d**y** at the inside of the curve to *(R+d)*d**y** at the outside, being *R* the radius of curvature and *d* the inner pipe diameter.

$$dL = R\,d\psi + \frac{d}{2}d\psi + \frac{d}{2}\cos\varphi\,d\psi$$

An infinitesimal strip area of the inner pipe wall is:

$$dA = dL\cdot\frac{d}{2}d\varphi = \frac{d}{2}\cdot[R+\frac{d}{2}(1+\cos\varphi)]\,d\psi\,d\varphi$$

The component of the force generated by the pressure on *dA* in the outward later direction is $dFv = p\,dA\cos\varphi$ and integrating this over the entire circumference leads to the net outward lateral force:

$$Fv\,ds = 2\cdot\int_0^{\pi} p\,\frac{d}{2}\cdot[R+\frac{d}{2}(1+\cos\varphi)]\cos\varphi\,d\psi\,d\varphi$$

which, for small deflections, using the relation:

$$\frac{d\psi}{ds} = \frac{1}{R} = -\frac{d^2y}{dx^2}$$

give total force F_v by unit length, generated at any cross section of the control element by the pressure on the pipe wall:

$$Fv = -\frac{\pi}{4}d^2p\frac{d^2y}{dx^2} \qquad (1)$$

It's worth noticing here how the contained fluid exerts a net lateral force on a deflected pipe. Its magnitude, per unit length, is the product of pressure, wet cross-section, and curvature. It acts towards the outside of the curve.
Another physical interpretation [3] of Eq.(1) is shown in Fig.(3) by isolating a fluid element within the pipe and resolving the net force component perpendicular to its axis.

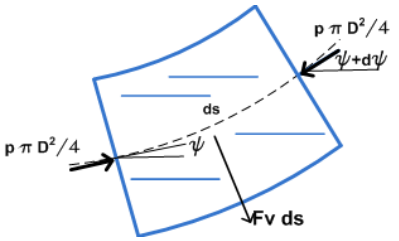

Fig.[3]: forces on a fluid element

From the equilibrium of the element in Fig.(2), being y small and ignoring the second order terms, we obtain:

$$q = -\frac{dV}{dx} - F_v + N\frac{d^2y}{dx^2}$$

for the transverse force balance and:

$$V = \frac{dM}{dx}$$

for the moment equilibrium.

We will consider hereafter slender pipes, without limitations to their wall thickness: their diameter is assumed small compared to the length. Hence, for the transverse beam deflection, we will neglect the shear components and limit our analysis to bending. Again, for small deflections, the bending stiffness relation:

$$E\,J\frac{d^2y}{dx^2} = -M$$

with the equilibrium relations above give:

$$E\,J\frac{d^4y}{dx^4} + P\frac{d^2y}{dx^2} = q \qquad (2)$$

Eq.(2) is identical to the equation governing a beam carrying a lateral load *q* and an axial compressive load *P* given by:

$$P = N + \frac{\pi}{4} d^2\, p \tag{3}$$

with *J* the bending moment of inertia of the pipe wall cross section *S* and *E* the elastic Young's modulus, assumed in the axial direction in case of a non isotropic material, and the normal force *N* on the pipe wall given by:

$$N = -\int_{Sbeam} \sigma_l \, dS \tag{4}$$

with σ_l the longitudinal stress due to the pressure induced tension in the end constrained pipe through the material Poisson ratio.

Eq.(2) rewritten as:

$$\frac{d^4 y}{dx^4} + \frac{P}{E\,J}\frac{d^2 y}{dx^2} = \frac{q}{E\,J} \tag{5}$$

has solution in the form of:

$$y = A'\sin(k\,x) + B'\cos(k\,x) + C'\,x + D' + \frac{q\,x^2}{2\,P}$$

with: $k^2 = P / E\,J$

and *A', B', C', D'* constants depending on the boundary conditions. Imposing now the four following conditions for built-in ends:

$$y = \frac{d\,y}{d\,x} = 0 \quad at\ x = 0\ and\ x = L$$

We obtain the values for the constants:

$$A' = \frac{qL}{2Pk} \qquad B' = \frac{qL}{2Pk}\,\frac{\sin(kL)}{1-\cos(kL)}$$

$$C' = -A'k = -\frac{qL}{2P} \qquad D' = -B' = -\frac{qL}{2Pk}\,\frac{\sin(kL)}{1-\cos(kL)}$$

and the solution of (5) for the deflection at middle span is[*]:

$$y(L/2) = \frac{qL}{2Pk}\left[\frac{1-\cos(k\,L/2)}{\sin(k\,L/2)} - \frac{k\,L}{4}\right] \tag{6}$$

Eq.(6) grows unbounded[†] for $k\,L/2 = \pi$ and thus for:

$$P = P_{crit} = \frac{4\,\pi^2 E\,J}{L^2} \tag{7}$$

Eq.(6) is then valid until $P = P_{crit}$ given by Eq.(7) where the solution diverges identifying the bifurcation instability point (buckling).

Solutions to Eq.(5) can be obtained in a similar way for all different cases of boundary conditions at the ends.

In the analysis that follows, being Eq.(2) and (3) still applicable for any type of material and pipe wall thickness, we will focus on the terms defining *P* in Eq.(3) and more specifically on σ_l. The relation between internal pressure and longitudinal stress is evaluated for a straight pipe configuration with built-in ends, giving plane strain conditions ($\varepsilon_l = 0$).

THIN ISOTROPIC PIPES

Consider now a thin isotropic pipe. From the Hooke's law for isotropic cylinders:

$$\varepsilon_l = \frac{1}{E}(\sigma_l - \nu(\sigma_c + \sigma_r) \tag{8}$$

With $\varepsilon_l = 0$ and because of the thin walled $\sigma_r = 0$ and $\sigma_c = \frac{p\,D}{2\,t}$ with *D* outer pipe diameter and *t* wall thickness, thus:

$$\sigma_l = -\nu\,\sigma_c = -\nu\,\frac{pD}{2t}$$

and Eq.(3), for $d \approx D$ and $S = \pi\,D\,t$ becomes:

$$P = \frac{\pi}{4} D^2\, p(1-2\nu) \tag{9}$$

and will result always compressive $P \geq 0$ since for isotropic materials $\nu \leq 0.5$.

Being *P* always positive, any applied internal pressure will cause an initially bent pipe to bend more. The additional bending will gradually increase till the internal

[*] Another way of coming to the solution (6) is from Timoshenko's "Theory of elastic stability" [1] where we can derive the equations of the deflection for a beam column with built in ends. The deflection curve equation is there given by the superposition of the two deflections due to the longitudinal load *P* with the lateral load *q* and from the effects (end moments) of the built in ends.

[†] Eq (5) has the classic solution of a beam column buckling [1] with: $P_{crit} = \pi^2 E\,J / l_k^2$ where l_k is buckling length which depends on the boundary conditions; for fixed ends $l_k = L/2$. To determine the critical load of a buckled bar equation (5) must be solved with the lateral load vanishing (homogeneous solution with *q*=0) and with the opportune boundary conditions at the ends

pressure reaches the critical value given by Eq.(7) and (9) with $J = \frac{\pi \cdot D^3 \cdot t}{8}$

$$p_{crit} = \frac{2\,\pi^2\,E\,D\,t}{(1-2\nu)\,l^2} \tag{10}$$

at which the pipe will become instable under the internal pressure (as a column) and buckle.

A qualitative plot of Eq.(6) using Eq.(9) above is depicted in Fig.(4) below.

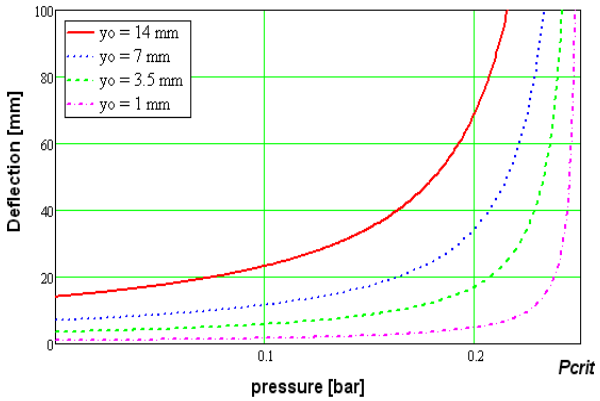

Fig.[4]: deflection Eq.(6) as function of the internal pressure p for different values of the initial deflection.

Fig.(4) shows that the pipe exhibits in fact the typical behaviour of a compression column buckling, with a clear dependency from the initial defect (initial curvature given by the lateral load *q*) and with the deflection becoming infinitely large in approaching the instability bifurcation point at the critical pressure.

In reality as we'll see later in the Finite Element Analysis, the large deformations effects together with the stress stiffening will limit the deflections to finite values and the overall sag at instability will be much less pronounced.

It can be easily shown that in case the pipe is also longitudinally pre-tensioned, meaning that the tension was applied before fully constraining the ends, the compressive force *P* becomes:

$$P = \frac{\pi}{4} D^2\,p\,(1-2\nu) - T \tag{11}$$

and the critical internal pressure is:

$$p_{crit} = \frac{2\,\pi^2\,E\,D\,t}{(1-2\nu)\,l^2} + \frac{T}{\frac{\pi}{4} D^2\,(1-2\nu)} \tag{12}$$

hence increasing or decreasing the bifurcation point pressure according to the sign of T.

THICK ISOTROPIC PIPES

From the Hooke's law Eq.(8), with $\varepsilon_l = 0$, the stress σ_l generated through the Poisson effects is:

$$\sigma_l = \nu(\sigma_c + \sigma_r)$$

from the equations for thick isotropic cylinders we know that the sum of the circumferential and radial stresses are constant at any radius of the pipe section:

$\sigma_c + \sigma_r = const = 2\sigma_m$ and $\sigma_m = \frac{p}{(\frac{b}{a})^2 - 1}$

with *a* inner pipe radius, *b* outer radius. It follows that:

$$\sigma_l = -\nu\,2\sigma_m = -2\nu\frac{p}{(b/a)^2 - 1} = -2\nu\,p\frac{(D-2t)^2}{D^2 - (D-2t)^2} \tag{13}$$

Introducing now the above expression with: $S = \pi(D-t)t$ into Eq.(4) we obtain:

$$P = \frac{\pi}{4}(D-2t)^2\,p\,(1-2\nu) \tag{14}$$

This is formally identical to equation (9) in terms of dependency upon the Poisson ratio.

The same conclusions as for thin pipes are then valid for thick isotropic pipes.

THIN ORTHOTROPIC PIPES

The Hooke's law for orthotropic cylinders is given by:

$$\begin{aligned}
\varepsilon_r &= \frac{\sigma_r}{E_r} - \nu_{cr}\frac{\sigma_c}{E_c} - \nu_{lr}\frac{\sigma_l}{E_l} \\
\varepsilon_c &= -\nu_{cr}\frac{\sigma_r}{E_r} + \frac{\sigma_c}{E_c} - \nu_{lc}\frac{\sigma_l}{E_l} \\
\varepsilon_l &= -\nu_{rl}\frac{\sigma_r}{E_r} - \nu_{cl}\frac{\sigma_c}{E_c} + \frac{\sigma_l}{E_l}
\end{aligned} \tag{15}$$

Under the usual assumptions $\varepsilon_l = 0$. Again for thin cylinders $\sigma_r = 0$. Equations (15) transform in:

$$\begin{aligned}
\varepsilon_r &= -\nu_{cr}\cdot\frac{\sigma_c}{E_c} - \nu_{lr}\cdot\frac{\sigma_l}{E_l} \\
\varepsilon_c &= +\frac{\sigma_c}{E_c} - \nu_{lc}\cdot\frac{\sigma_l}{E_l} \\
0 &= -\nu_{cl}\cdot\frac{\sigma_c}{E_c} + \frac{\sigma_l}{E_l}
\end{aligned}$$

And the last gives:

$$\sigma_l = \nu_{cl} \cdot \frac{E_l}{E_c} \sigma_c$$

which with the reciprocity relation:

$$\nu_{lc} = \nu_{cl} \cdot \frac{E_l}{E_c}$$

becomes:

$$\sigma_l = \nu_{lc}\, \sigma_c \tag{16}$$

and with $\sigma_c = \frac{p\,D}{2\,t}$ for thin cylinders, we obtain:

$$P = \frac{\pi}{4} D^2 p (1 - 2\nu_{lc}) \tag{17}$$

It is interesting to notice here that the term s_l in Eq.(4) is driven by the Poisson ratio ν_{lc} and that P now fully depends on that parameter.

Orthotropic cylinders as laminate composites can manifest values of ν_{lc} well above 0.5. When for instance we take a soft composite like a $[+\theta/\text{-}\theta]$ angle ply laminate[‡], we see in Fig.(5) that varying the ply angle, the Poisson ratio ν_{lc} can be larger than 2 and remain above 0.5 for theta angles up to about 55 deg.

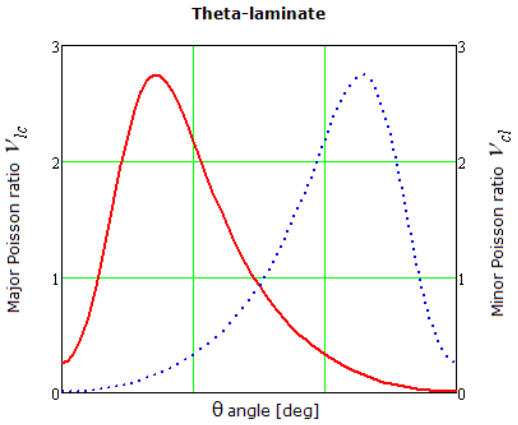

Fig.[5]: Theta-plot of the Poisson ratio's calculated for a nylon fibres - PVC plasticized matrix theta-laminate; (Ef=3300MPa; Vf=20%; Em=5MPa)

In this case it becomes clear that an orthotropic material pipe may exhibit the opposite behaviour of an isotropic one. With values of $\nu_{lc} > 0.5$, P in Eq.(17) becomes negative, thus tensile, meaning that the pressure induced longitudinal stress through the high Poisson ratio prevail on the pressure induced bending effects.

[‡] As in the case of cord-rubber as some pressure hose pipe. Similar effects can also be found in epoxy/T300 laminates for winding angles between 15-55 deg. [8]

The initial pipe deflection is expected to decrease with the pressure rising inside the pipe.

The curves of Fig.(5) can be obtained by the approximated formulas reported by Tsu-Wei Chou [7]:

$$\nu_{lc} = \frac{E_f V_f \sin^2\theta \cos^2\theta + 2\,\frac{G_m}{1-V_f}}{E_f V_f \sin^4\theta + 4\,\frac{G_m}{1-V_f}} \tag{18}$$

Where E_f and V_f are the elastic modulus and volume of the fibers, G_m is the shear modulus of the matrix. These formulas and dedicated tools as Esacomp™[§] allow designing angle ply composites with Poisson ratio's well above 0.5, thus stable under internal pressure.

The above effects have been simulated by the Finite Element Analysis described further on. Numerical results are in very good agreement with Eq.(17).

From Eq.(16) one can also conclude that the longitudinal pipe wall stress is:

$$\sigma_l = \nu_{lc}\, \sigma_c = \nu_{lc}\, \frac{p\,D}{2\,t} \tag{19}$$

and that for a given pipe with internal pressure it is always positive (pull out) and proportional to the Poisson ratio.

THICK ORTHOTROPIC PIPES

From the Hooke's law for orthotropic cylinders Eq.(15) with $\sigma_r, \sigma_c, \sigma_l \neq 0$ and $\varepsilon_l = 0$ we obtain:

$$\sigma_l = E_l \left(\nu_{rl} \frac{\sigma_r}{E_r} + \nu_{cl} \frac{\sigma_c}{E_c}\right) \tag{19}$$

and from the reciprocity relations:

$$\sigma_l = \nu_{lr} \cdot \sigma_r + \nu_{lc} \cdot \sigma_c \tag{20}$$

which is the same of Eq.(16) for thin orthotropic cylinders with the additional term $\nu_{lr}\, \sigma_r$

In case we take for instance the orthotropic flexible composite of Fig.(5), we can assume that due to the rubber matrix the composite is uncompressible thus, for small strains we have $\varepsilon_l + \varepsilon_r + \varepsilon_c = 0$, providing:

$$\nu_{lr} = -\frac{\varepsilon_r}{\varepsilon_l} = 1 + \frac{\varepsilon_c}{\varepsilon_l} = 1 - \nu_{lc}$$

And equation (20) above becomes:

[§] ESAComp is a software for the analysis and design of composite laminates and laminated structural elements.

$$\sigma_l = (1-\nu_{lc}).\sigma_r + \nu_{lc}\sigma_c$$

or:
$$\sigma_l = \sigma_r - \nu_{lc}(\sigma_r - \sigma_c) \qquad (21)$$

which can be developed further with the expressions for anisotropic cylinders [6,10] where:

$$\sigma_r(r) = \frac{p\,a^{n+1}}{b^{2n}-a^{2n}}\cdot(r^{n-1} - b^{2n}r^{-n-1})$$
$$\sigma_c(r) = \frac{n\ p\,a^{n+1}}{b^{2n}-a^{2n}}\cdot(r^{n-1} + b^{2n}r^{-n-1}) \qquad (22)$$

$$n = \sqrt{\frac{E_\theta}{E_r}}$$

with *n* index of anisotropy of the material.

The longitudinal force on the pipe wall is then given by Eq.(4):

$$N(p) = -2\pi\int_a^b \sigma_l(r)\, r\, dr \qquad (23)$$

And thus the overall compression/tension force *P*:

$$P = \frac{\pi}{4}(D-2t)^2\, p + N(p) \qquad (24)$$

that can be used in Eq.(6) to compute the deflection and also determine the critical pressure *p* when equating to *Pcrit* given by Eq.(7).

From numerical examples one can note that despite Eqs.(21) are approximations based on small strains and material incompressibility, their use with Eq.(23) provides better results than simply adopting Eq.(14) with $\nu=\nu_{lc}$.

NUMERICAL ANALYSIS OF ORTHOTROPIC PIPES

A finite element model was developed in the Ansys™ parametric design language (APDL).
The elements used are Shell181 (for thin pipes) with the introduction of large deformations[**] and stress stiffening effects.
To understand how the Finite Element Model can take into account the coupling between fluid pressure and curvature, we should refer to the control element of Fig.(1). Not only a large deformation analysis is required for the pressure to follow the deformed pipe geometry at each iteration, but the elements must have large strain capabilities to account for the fibres elongation at the bottom of the pipe and thus for the increased surface and load from the pressure.
The choice of Shell181 elements (large rotation and large strain capability), resulted then fundamental to account for the coupling effects above.

In order to simulate various Poisson ratio's for orthotropic materials, a composite pipes like the two-ply theta laminate of Fig.(5), was selected for the simulations.

When modelling composite layers, elements in Ansys are rotated and oriented according to the Esacomp conventional reference system Fig.(6):

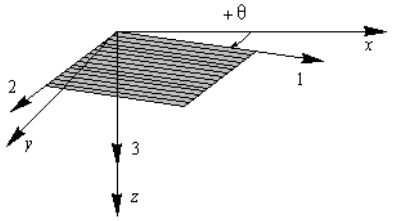

Fig.[6]: ply and laminate reference system

Fig.(6) shows the three directions defining the principle axes of the reinforced ply. The laminate local coordinates x,y,z correspond in the Ansys model to the longitudinal, circumferential and radial directions.

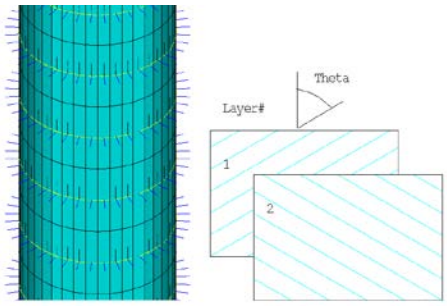

Fig.[7]: Ansys model showing the element coordinate system (x longitudinal, y circumferential, z radial). Example of two-ply theta laminate ±60 deg.

The following single ply engineering constants have been provided in input for each layer:

E_1	MPa	664	ν_{12}	--	0.402
E_2	MPa	6.25	ν_{23}	--	0.42
E_3	MPa	6.25	ν_{13}	--	0.402
G_{12}	MPa	2.2			
G_{23}	MPa	2.2			
G_{13}	MPa	2.2			

Table [1]: Single ply elastic constants for nylon cord/PVC reinforced ply ; Vf=20% ; Em=5 MPa; nu_m=0.42; Ef=3300 MPa; nu_f=0.33, t=1.1 mm

[**] *When introducing large deformation effects, Shell181 elements include automatically stress stiffening. Other elements tested in the analysis as shell43 and solid46, allowing the input of orthotropic material properties, large deformations with and without stress stiffening effects) were showing a consistent but slightly stiffer behaviour. No reliable results were obtained with shell63 elements.*

The full laminate characteristics were firstly calculated using Esacomp Fig.(8). The corresponding laminate elastic properties were then targeted in the finite element analysis by changing parametrically the theta angle orientation.

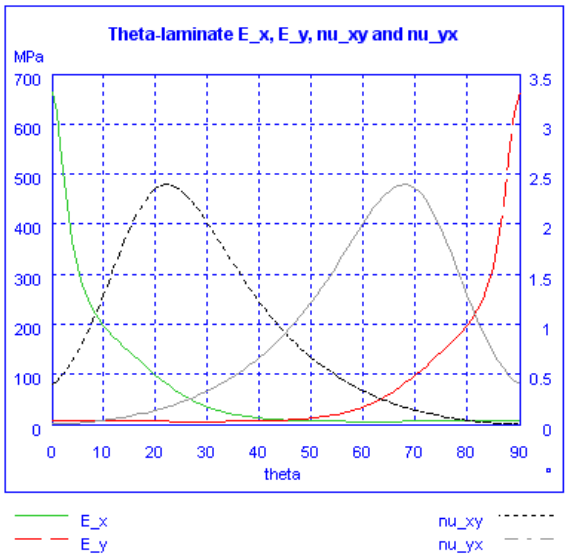

Fig.[8]: Esacomp theta-plot of the engineering parameters calculated for the nylon fibres-PVC plasticized matrix theta-laminate.; Layup +theta/-theta. Created with ESAComp 3.5 using Standard micromechanics analysis.

The code was run for pipe geometries with a mean diameter of 16 mm, 2.2 mm wall thickness, 2 m length, with built-in ends. When looking for a comparison with the equations of the previous sections, the pipe density was varied to control the initial gravitational sag and maintain the analysis in the range of the small displacement.

Several runs have been performed and results are summarized here below.

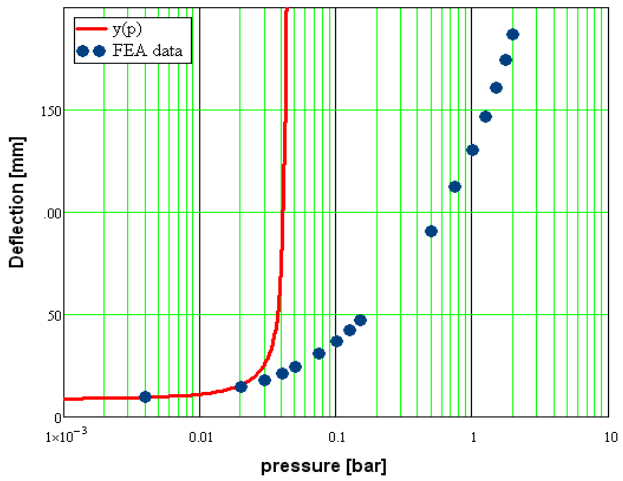

Fig.[9] logarithmic scale plot of the numerical results compared to thick pipe equations(6 and 24); theta ±60 deg; ν_{lc} = 0.332; initial deflection 9.5 mm; increased bending with pressure.

The plot of Fig.(9) shows the increased bending with pressure for a pipe laminate with theta ±60 deg and ν_{lc}=0.332 from an initial deflection of 9.5 mm given by the lateral load.
The analytical curve (in red) from Eqs.(6,24) shows a good matching with the FEA results in the range of small deformations till the stability limit where the small deflection theory breaks down and where instead the large deformation approach of the FEA provide a determinate solution due as well to a to noticeable stress stiffening.

Fig.(10,11) below shows the same analysis done for a laminate with theta ±45 deg, ν_{lc} = 0.910 and for initial deflections of 6.9 mm and 40 mm. It is evident there the straightening of the pipe with pressure as well as the very good matching of results for small deflections.

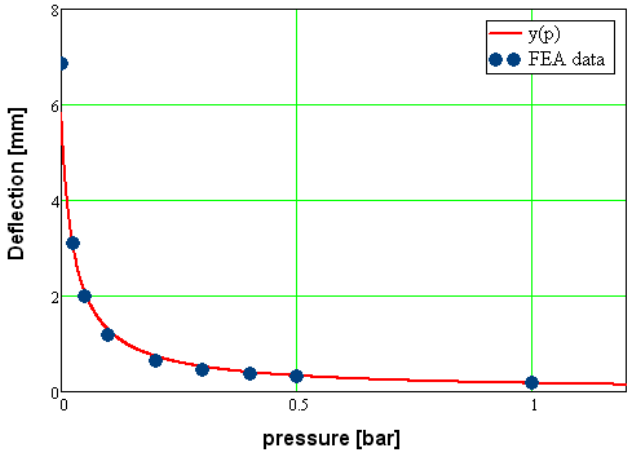

Fig.[10] Numerical results compared to thick pipe equations(6 and 24); theta ±45 deg; ν_{lc} = 0.9105.; initial deflection 6.9 mm; pipe straightening with pressure

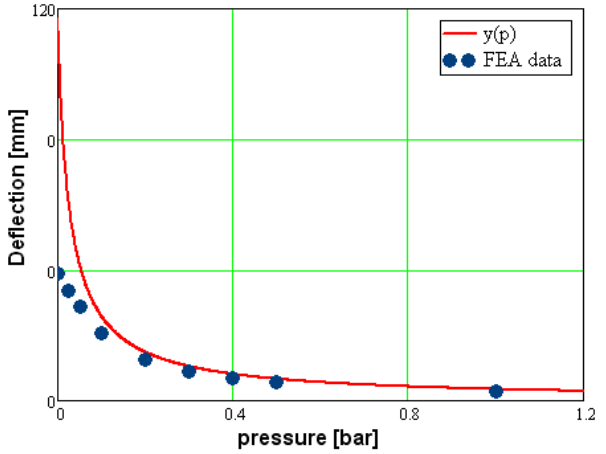

Fig.[11] Numerical results compared to thick pipe equations(6 and 24); theta ±45 deg; ν_{lc} = 0.9105; initial deflection 40 mm ;showing mismatch at large deflections between analytical curve and FEA.

The plots above show that the Ansys model can predict well the opposite effects of either straightening or increased bending for the laminate of Fig.(8) when ν_{xy} = ν_{lc} is respectively higher or lower than ½. This happens for

theta > 54.3[††] as can be calculated by the micromechanics analysis used by Esacomp and Ansys. The plot of Fig.(12) below shows well the inversion of the pipe behaviour around that value.

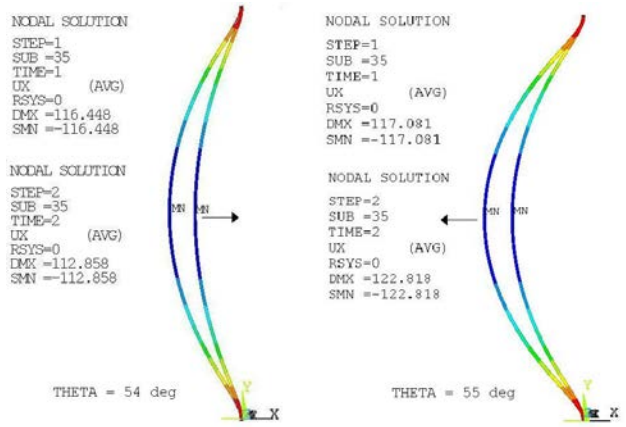

Fig.[12] Initial bending under gravity and stretching (theta = ±54 deg) or increased bending (theta = ±55 deg) with 1 bar internal pressure. Amplification factors between 3.5 and 4 applied.

CONCLUSIONS

Isotropic material pipes under internal pressure will buckle laterally once the pressure approaches the critical value. When initially curved they will bend progressively more till sudden instability. These effects on a curved pipe are due to the lateral force transmitted to the pipe wall by the internal pressure, which acts towards the outside of the curve and always prevails on the pressure induced tension through the material Poisson ratio in the end constrained pipe.

When the material is orthotropic, depending on the orientation and the elastic properties given by the constituent matrix and fibres, the effects of internal pressure can generate an opposite behaviour with the pipe getting straighter.

In both cases the Poisson ratio plays a fundamental role with the expression defining the sign of the axial compression force *P* on the pipe, given by:

$$P = const \cdot p \cdot (1 - 2\nu)$$

For isotropic material Eqs. (9,14), being $\nu \le 0.5$, the axial force results always compressive $P \ge 0$ generating bending and instability whereas for some orthotropic materials Eq.(17,24) $\nu = \nu_{lc}$ can exceed the value of 0.5 reversing thus the sign of *P* and causing the straightening the pipe.

These effects have also been tested in the lab with good qualitative matching.

[††] This angle [7] is close to the predicted "magic angle" of 54.7 deg for a unidirectional cord/rubber composites where the stretch-shear coupling γ_{xy} vanishes (being negative before and positive after). This is not observed in rigid composites.

ACKNOWLEDGEMENTS

I would like to thank my colleagues Hans Danielsson and Piet Wertelaers for the technical discussions and for reviewing this article.

REFERENCES

[1] S.P. Timoshenko, J.M. Gere, *Theory of elastic stability*. Second edition.
[2] J.A. Haringx , *Instability of thin-walled cylinders subjected to internal pressure.* Philips Research, Reports , Vol.7 , 1952, pp.112-118.
[3] A.C. Palmer, *Lateral buckling of axially constrained pipelines*. JPT Journal of Petroleum Technology, Forum Nov. 1974, pp.1283-1284.
[4] M. Motavalli et al., *Buckling of polymer pipes under internal pressure*. Materials and Structures, 1993, 26, pp. 348-354.
[5] D.S. Burnett, Chung-Chun Ong, *Shortening of Submerged Ocean cables Due to Hydrostatic pressure*. IEEE Journal of Oceanic Engineering, Vol OE-12, No. 1, January 1997, pp. 281-288.
[6] D. Gal, J. Dvorkin, *Stresses in Anisotropic Cylinders*. Mechanics Research Communications, Vol 22, No. 2, 1995, pp. 109-113.
[7] Tsu-Wei Chou, *Review of Flexible Composites.* Journal of Material Science 24, 1989, pp. 761-783.
[8] M. Xia et al., *Analysis of filament wound fiber reinforced sandwich pipe under combined internal pressure and thermo-mechanical loading*. Elsevier, Composites Structures 51 (2001), pp. 273-283.
[9] L.D. Peel, *Investigation of High and Negative Poisson's Ratio Laminates.* P97.
[10] M. Suchanek, J. Vrbka, *Stress and strain modeling in the orthotropic wound part of high pressure compound vessels*, Elsevier, International Journal of Pressure Vessels and Piping, 77 (2000), pp. 289-295.
[11] P.K. Mallik, *Fiber-Reinforced Composites.* Second edition.